Phylogenetic and Environmental Diversity Revealed for Tournaisian Tetrapods

Clack, J. A[1]., Bennett, C. E[3]., Carpenter, D. K[4]., Davies, S. J[3]., Fraser, N. C[5]., Kearsey, T. I[6], Marshall, J. E. A[4]., Millward, D[6]., Otoo, B. K. A[1,2]., Reeves, E. J[4]., Ross, A. J[5]., Ruta, M[7]., Smithson, K. Z[1]., Smithson, T. R[1]. & Walsh, S. A[5].

Author Affiliations

[1]J. A. Clack, K. Z. Smithson, T. R. Smithson, [1,2]B. K. A. Otoo† University Museum of Zoology, Cambridge, Downing St., Cambridge CB2 3EJ, UK

[3]C. E. Bennett, S. J. Davies, Department of Geology University of Leicester, Leicester, LE1 7RH, UK

[4]D. K. Carpenter, J. E. A. Marshall, E. J. Reeves, National Oceanography Centre, University of Southampton, Waterfront Campus, European Way, Southampton, SO14 3ZH, UK

[5]N. C Fraser, S. Walsh, A. J. Ross, National Museum of Scotland, Chambers St., Edinburgh, EH1 1JF, UK

[6]T I. Kearsey, D. Millward, British Geological Survey, The Lyell Centre, Research Avenue South, Edinburgh, EH14 4AP, UK

[7] M. Ruta, School of Life Sciences, University of Lincoln, Joseph Banks Laboratories, Green Lane, Lincoln LN6 7DL, UK

†current address, [2]School of Earth Sciences, University of Bristol, Bristol, BS8 1RJ, UK

Summary

The end-Devonian to mid-Mississippian time interval has long been known for its depauperate palaeontological record, especially for tetrapods. This interval encapsulates the time of increasing terrestriality among tetrapods, but only two Tournaisian localities previously produced tetrapod fossils. Here we describe five new Tournaisian tetrapods from two localities and their environmental context. A phylogenetic analysis retrieved three of these taxa as stem tetrapods, interspersed among Devonian and Carboniferous forms, and two as stem amphibians, indicating a deep split among crown tetrapods. The new taxa suggest that tetrapod diversification was well established by the Tournaisian. Sedimentary evidence indicates that coastal plain monsoonal wetlands provided a fluctuating regime of alternating drier and wetter habitats potentially conducive to the radiation of tetrapods. We show that atmospheric oxygen levels were stable across the Devonian/Carboniferous boundary, and did not inhibit the evolution of terrestriality. This wealth of tetrapods from new Tournaisian localities indicates the likelihood of new discoveries elsewhere.

The term "Romer's Gap" was coined[1,2] for a hiatus in the fossil record of tetrapods from the end-Devonian to the Mid-Mississippian (Viséan), an interval of approximately 25 million years (Myr)[3]. Following the end-Devonian, the earliest terrestrial tetrapod fauna was known from the Brigantian (late Viséan) locality of East Kirkton near Bathgate, Scotland[4,5]. By that time, tetrapods were ecologically diverse, exploited a wide range of niches, and were terrestrially capable. With five or fewer digits, some had gracile limbs [6,7], unlike the polydactylous aquatic or semi-aquatic fish-like tetrapods of the Late

47 Devonian [8]. Fossil evidence of the transitional forms between these disparate
48 morphologies was almost entirely lacking, confounding efforts to understand the
49 acquisition of terrestrial characteristics by tetrapods, or the relationships between the
50 already diverse mid-Carboniferous tetrapod groups. Alternative hypotheses to explain
51 this hiatus have included a low oxygen regime during the earliest Carboniferous [9] or
52 lack of appropriate or successful collecting in Tournaisian strata [2].

53 The few isolated tetrapod limb and girdle elements and numerous tetrapod
54 trackways from the Tournaisian of the Horton Bluff Formation at Blue Beach and
55 Horton Bluff, Nova Scotia, have not been fully described [10,11]. The only other
56 Tournaisian tetrapod material was the articulated skeleton of *Pederpes finneyae*, from
57 the Tournaisian Ballagan Formation (Inverclyde Group) near Dumbarton, western
58 Scotland [12,13]. More recently, new taxa from this formation in the Borders Region of
59 Scotland were reported [2], initiating a NERC-funded consortium programme to study that
60 formation and its fauna, alongside environmental and climatic data.

61 We report here on some of our major findings. They show that far from being
62 almost devoid of tetrapods, the Tournaisian included a rich and diverse assemblage of
63 taxa. These include close relatives of some Devonian forms on the tetrapod stem, and
64 basal members of the amphibian stem. We diagnose and name five taxa (Figs 1-4), and
65 briefly summarize at least seven other taxa that are distinct but undiagnosable at present
66 **(Extended Data Figs 1-6)**. This level of diversity matches that recently recorded for
67 Tournaisian lungfish and chondrichthyans [14,15].

68 We also report findings on the environment of the Ballagan Formation in which
69 these tetrapods lived. The fauna occupied a closely juxtaposed mosaic of different

microhabitats with highly variable salinity and water levels driven by a sharply contrasting seasonal climate that persisted over the 12 million years of the Tournaisian3. We show that atmospheric oxygen levels were stable across the Devonian/Carboniferous boundary, and did not drop significantly enough to compromise terrestrial faunal life (contra ref 9). The Ballagan environments, varying between ponds, swamps, streams and floodplains, combined with floral changes following the end-Devonian, are here considered important factors driving tetrapod evolution.

Tetrapoda Goodrich, 1930 indet.

Perittodus apsconditus gen. et sp. nov. Figure 1 e-g.

Smithson et al., 2012 (fig. 4), new taxon A.

Zoobank ID tbc

Etymology. Genus from *perittos* (Greek) 'odd' and *odus* (Greek) 'tooth' referring to the unusual dentition of the mandible. Species from *apsconditus* (Latin) 'covert, disguised, hidden, secret or concealed', referring to the fact that it was only discovered by micro-CT scanning.

Holotype. UMZC 2011.7.2 a and b. Cheek region of skull, lower jaw, and scattered postcranial elements in part and counterpart.

Locality and Horizon. "Willie's Hole", Whiteadder Water near Chirnside. Ballagan Formation. Early mid Tournaisian.

Diagnosis. *Perittodus apsconditus* differs from all other tetrapods in the following combination of autapomorphic and derived characters. Autapomorphies: unique adsymphysial and coronoid dentition – adsymphysial with two tusks and at least two smaller teeth, anterior coronoid with two or three larger tusks, middle coronoid with two larger and two or three smaller teeth, posterior coronoid row of small teeth; lozenge-

shaped dorsal scales bearing concentric ridges centred close to one edge nearer to one end. Derived characters: deeply excavated jugal with narrow suborbital bar (earliest known occurrence of this feature); lateral line an open groove on jgal.

Attributed specimen. UMZC 2016.1. Isolated dentary and adsymphysial (in micro-CT scan) from cliffs at the Ross end of Burnmouth, 373.95 m above the base of the Ballagan Formation. Early mid Tournaisian.

Remarks: Lower jaw length 68 mm. Maxilla of holotype visible in micro-CT scan.

Koilops herma gen. et sp. nov. Fig. 1 a-b.

Smithson et al., 2012 (fig. 2C), 'probable new taxon'.

Zoobank ID tbc

Etymology. Genus from *koilos* (Greek) 'hollow or empty', and *ops* (Greek) 'face', referring to the skull mainly preserved as natural mould. Species from *herma* (Greek) 'boundary marker, cairn, pile of stones'. The specimen, from the Borders Region of Scotland, has transitional morphology between Devonian and Carboniferous tetrapods.

Holotype. NMS G. 2013.39/14. Isolated skull mainly as a natural mould.

Locality and Horizon. "Willie's Hole", Whiteadder Water near Chirnside. Ballagan Formation. Early mid Tournaisian.

Diagnosis. *Koilops herma* differs from all other tetrapods in the following combination of autapomorphic and derived characters. Autapomorphies: fine irregular dermal ornament with conspicuous curved ridges around the parietal foramen and larger pustular ornament anterior to parietal foramen. Derived characters: deeply excavated jugal with narrow suborbital bar; large parietal foramen.

Remarks. Skull length 80 mm. The dermal bones are robust and well integrated so the individual was almost certainly not a juvenile.

Ossirarus kierani gen. et sp. nov. Fig. 2.

Zoobank ID tbc

Etymology. Genus from *ossi* (Latin) 'bones' and *rarus* (Latin) 'scattered or rare.' Specific name to honour Oliver and Betty Kieran, residents of Burnmouth, who have supported us throughout our work, and encouraged the interest and co-operation of the Burnmouth community.

Holotype. UMZC 2016.3. A single block containing scattered skull and postcranial remains.

Locality and Horizon. Cliffs at the Ross end of Burnmouth, 340.5 m above the base of the Ballagan Formation. Mid Tournaisian.

Diagnosis. *Ossirarus kierani* differs from all other tetrapods in the following combination of autapomorphic and derived characters. Autapomorphies: tabular elongate triangle forming a conspicuous tabular horn with a convex lateral margin. Derived character: tabular-parietal contact (earliest known occurrence of this feature). Exoccipital separate from basioccipital (earliest known occurrence of this feature).

Remarks. Estimated skull length 50 mm based on comparisons with *Acanthostega*, *Ichthyostega* and *Greererpeton* [16-18].

Diploradus austiumensis gen. et sp. nov. Fig. 3.

Zoobank ID tbc

Etymology. Genus from *diplo* (Greek) 'double' and *radus* (Greek) 'row' referring to the double coronoid tooth row. Species from *austium* (Latin) 'mouth of a river or stream' referring to Burnmouth.

144 **Holotype.** UMZC 2015.55.4. Small disrupted skull with lower jaw, palate and skull
145 roofing bones.
146 **Locality and Horizon.** Cliffs at the Ross end of Burnmouth, 373.95 m above the base of
147 the Ballagan Formation. Mid Tournaisian.
148 **Diagnosis.** *Diploradus austiumensis* differs from all other tetrapods in the following
149 combination of autapomorphic and derived characters. Autapomorphies: lower jaw with
150 irregular double row of denticles along the coronoids; around 51 dentary teeth and
151 spaces, with enlarged tusk at position 3 and the largest teeth in positions 8-13; parietals
152 short, pineal foramen anteriorly placed; ?narrow curved pre- and postfrontals. Derived
153 characters: deeply excavated jugal with narrow suborbital bar; parasphenoid with broad,
154 flattened posterior portion with lateral wings (earliest known occurrence of a
155 parasphenoid crossing the ventral cranial fissure), cultriform process flat, narrow.
156 **Attributed specimen**. UMZC 2016.4 a and b. The anterior end of a mandible from 341
157 m above the base of the Ballagan formation at Burnmouth.
158 **Remarks.** Lower jaw length 30 mm. It superficially resembles that of *Sigournea* [19],
159 although a relationship is not supported by cladistic analysis. The thinness of the bones
160 and their distribution suggest a juvenile.
161
162
163 ***Aytonerpeton microps*** gen. et sp. nov. Fig. 4.
164 Zoobank ID tbc
165 **Etymology.** Genus name from Ayton, the parish in the Scottish Borders from which the
166 specimen came, and *erpeton* (Greek) ‘crawler’ or ‘creeping one’. Species name from
167 *micro* (Greek) ‘small’ and *ops* (Greek) ‘face’.

Holotype. UMZC 2015.55.8. Partial skull and scattered postcrania visible only in micro-CT scan (**Supplementary Information 1 and 2, two movie files**)

Locality and Horizon. Shore exposure at the Ross end of Burnmouth, 340.6 m above the base of the Ballagan Formation. Mid Tournaisian.

Diagnosis. *Aytonerpeton microps* differs from all other tetrapods in the following combination of autapomorphic and derived characters. Autapomorphies: two enlarged premaxillary teeth plus one large tooth space at posterior end of premaxilla; 5 teeth on premaxilla; adsymphysial with a single tooth; coronoids apparently lacking shagreen; L-shaped lacrimal; vomer with at least one tooth, palatine with one large fang but lacking smaller teeth; ectopterygoid with at least two teeth and possible smaller teeth.

Remarks. Reconstructed skull length about 50 mm.

See **Supplementary Information 3** for plesiomorphies, characters of uncertain polarity, remarks and sedimentological context.

Results

Cladistic Analysis

A maximum parsimony analysis of a new data matrix (**Supplementary Data 4 Character list and Data matrix**) incorporating the five new Tournaisian taxa yielded 4718 shortest trees with all characters unordered and of equal unit weight. The strict consensus is very poorly resolved (Fig. 5, **Extended Data Fig. 7**), and only a handful of clades appear in more than half of all shortest trees. No taxon was considered suitable for safe taxonomic reduction [20]. Branch support is weak to moderate, although Tournaisian taxon topology stabilizes with increased implied weighting [21], which produced many fewer trees (Fig. 6a, b) and reveals novel features in the branching sequence of major early tetrapod groups. Three analyses with implied weighting were

run, each using a different value of the constant of concavity K [21] (**Methods and Extended Data Fig. 7**).

In these analyses, the relative positions of the new Tournaisian taxa are unaltered; crownwards, the branching sequence includes: *Ossirarus*, *Perittodus*, *Diploradus*, *Koilops*, and *Aytonerpeton*. Three taxa are placed below the node subtending crown tetrapods. *Ossirarus* is crownward of *Acanthostega*, *Ventastega*, and *Ichthyostega*, and is the most plesiomorphic taxon among Carboniferous tetrapods. *Perittodus* is sister-taxon to the Devonian *Ymeria*. *Diploradus*, though crownward of *Whatcheeria* and *Ossinodus,* occurs below the grade complex of *Crassigyrinus*, baphetids, and other taxa more proximal to the crown group node. In most analyses, *Koilops* and *Aytonerpeton* are placed on the amphibian stem – the latter within a *Tulerpeton*-colosteid clade – and may therefore be part of the tetrapod crown group [22-24, but see 25,26].

The new taxa force reassessment of the sequence of branching events in the tetrapod stem, with Carboniferous stem group positions sometimes altered substantially relative to previous studies [22-26]. Carboniferous and Devonian taxa interspersed along the stem may indicate the likelihood of a more ramified stem than previously suspected. Since *Aytonerpeton* and *Koilops* appear in the crown there may have been a deeper split between stem amphibians and stem amniotes than previously recognized.

Geology and Environment

The Ballagan Formation (Inverclyde Group) underlies much of the Midland Valley of Scotland and the northern margin of the Northumberland Basin. To interpret the environment, we obtained a 490 metre borehole core through the formation, located at

Norham near Berwick-Upon-Tweed (British National Grid Reference 391589, 648135), and logged the entire 520 m Burnmouth (396000-661000) succession at centimetre scale intervals (**Methods and Extended Data Fig. 1**). Both sections were subjected to sedimentary, palaeontological, palynological, isotope and charcoal analyses.

Deposited on a low-lying coastal floodplain during sedimentary basin initiation in central Scotland and northern England on the south-east margin of Laurussia [27-28], the Ballagan Formation comprises sandy siltstone, grey siltstone, and sandstone, with sporadic nodules and thin beds of ferroan dolostone ('cementstones')[29]. Previously little studied, the abundant palaeosols, sandy siltstones and thin evaporite deposits [30] provide crucial environmental information.

At Burnmouth the vertically dipping strata probably span the entire Tournaisian [2,31]. The stratigraphical position of the succession at Willie's Hole is inferred from a nearby borehole (Hutton Hall Barns, BGS Registered number NT85SE1: base proved at depth of 142.5 m), about 150 m above the base of the formation.

Floodplain environments are the most important sites for tetrapod fossil preservation in the Ballagan Formation. Although palaeosols are found at two Late Devonian tetrapod localities [32,33], our study is the first to record such a rich diversity of tetrapods from beds closely associated with palaeosols. The sandy siltstone deposits, which contain the highest fossil concentration of any sediment type in our study area [30] were deposited in seasonal, probably monsoonal, flooding events and commonly overlie palaeosols or desiccated surfaces [30]. The alternation of fossil-bearing siltstones with palaeosols indicates the abrupt switching between floodplains with high water tables and semi-permanent water bodies and drier floodplain environments (Fig. 6a). Tetrapods

240 within sandy siltstones may have originated in wet vegetated areas, small floodplain
241 lakes or pools. Whereas overbank sediments predominate, frequent cryptic localised
242 marine incursions could have acted as important pathways between marine, freshwater
243 and terrestrial habitats for animals. The common occurrence of tetrapods within the
244 monsoonal flood derived deposits[30] may indicate that they had achieved some measure
245 of terrestriality, living within the marsh-like wetland habitats, or in adjacent shallow
246 lakes.

247 Diplopoda (millipedes) were terrestrial [34], and demonstrate the existence of
248 terrestrial environments in the Ballagan Formation. Four articulated and generally well-
249 preserved helminthomorph diplopod specimens have been recovered, from Willie's Hole
250 and Burnmouth 2 (Fig 6b). Helminthomorphs are generally rare in the early
251 Carboniferous, but the new specimens, all different from each other, imply a high
252 diversity of terrestrial Tournaisian arthropods. Fossil scorpions, recovered from Willie's
253 Hole 2 (Fig 6c), Burnmouth, and Coquetdale (390150 606070), may or may not have
254 been terrestrial, but add to the diversity of Tournaisian arthropods.

255 Diversification of land plants in the early Carboniferous initiated a change in
256 fluvial and floodplain architecture [35-37] following the end-Devonian extinctions.
257 Progymnosperms were almost eliminated at the end of the Famennian, but thickets and
258 forests were re-established in the early-mid Tournaisian with lycopods as keystone taxa.
259 At Burnmouth many beds with abundant spores of the creeping lycopod *Oxroadia*
260 include tetrapods. The flora would have provided micro-habitats for arthropods, forming
261 a possible food supply for tetrapods. Dispersed spores from Willie's Hole suggest a
262 more stable forested landscape of arborescent lycopods.
263

Atmospheric oxygen levels in the Tournaisian

To address the low oxygen hypothesis[9] we examined fossil charcoal (fusain) in the Ballagan Formation to estimate atmospheric oxygen levels in the Tournaisian relative to both the Late Devonian and later Mississippian. Wildfire activity (and hence charcoal production) is proportional to oxygen supply[38-42]. It has been demonstrated that when O_2 exceeds the present atmospheric level (PAL) of 20.9%, fire activity rapidly increases and reaches a plateau at around 24% **(Methods**). It is strongly supressed below 20% O_2 and switched off completely below 16%, even in very dry conditions[43].

Charcoal, either as microscopic dispersed organic matter (DOM) or visible in hand specimens, is relatively common at Burnmouth and Willie's Hole. Although charcoal is reported from the Tournaisian Horton Bluff Formation, Nova Scotia[43] as indicating O_2 concentrations above 16%, no quantitative study to validate this result has been undertaken.

We analysed 127 rock samples collected from the Famennian of Greenland (Stensiö Bjerg Formation), the Tournaisian Burnmouth Shore section, and the Viséan of Fife, Scotland (Strathclyde Group) (**Extended Data Fig. 8 and Extended Data Table 1**). All were found to contain fusinite, with a mean abundance relative to total phytoclasts of 2.0%, 2.3% and 2.6% for the Famennian, Tournaisian and Viséan, respectively. We also analysed 12 samples from Willie's Hole which had a mean value of 2.0% **(Extended Data Table 1).** Not only do these results mean that fire activity persisted through Romer's Gap and indicate that atmospheric O_2 did not fall below 16%, but also that there was no significant change in charcoal production compared with the Famennian and Viséan (**Extended Data Fig. 8**). This strongly suggests that atmospheric

287 O_2 was stable across this time interval, refuting hypoxia as an explanation for Romer's
288 Gap.
289
290 **Discussion**
291 Our findings profoundly alter the prior perception of the earliest Carboniferous as a
292 hiatus in the vertebrate fossil record and challenge its interpretation as a depauperate,
293 low diversity interval for vertebrates. Although evidence of an extinction event at the
294 end of the Devonian shows the demise of many archaic fish groups [44], we are gaining
295 new perspectives on the recovery and diversification of surviving groups, which went on
296 to found the basis of modern vertebrate diversity.
297 The new tetrapods, spread across the tetrapod stem and into the crown group,
298 show no close relationship to each other, and exhibit different combinations of
299 plesiomorphic and derived characters. Some taxa cluster with Devonian forms,
300 suggesting a possible relict fauna, whereas others appear more crownward, even
301 clustering near the base of the crown group. They imply an early radiation of tetrapods
302 during the Tournaisian, and at the same time, suggest a blurring of the Devonian-
303 Carboniferous (D-C) boundary in respect of tetrapod evolution, a feature also noted in
304 tetrapod remains from Nova Scotia [45].
305 If confirmed, our results, imply a deep split between stem amphibians and stem
306 amniotes in the earliest Carboniferous. This accords with most molecular dates for the
307 split that place it at between 360 and 333 Ma, with an average of 355 Ma [46,47]. The
308 latter date, 4 Ma after the end-Devonian, suggests that the origin of the tetrapod crown
309 group occurred soon after the extinction event as tetrapods began to recover. Their

radiation into a range of new taxa parallels that of lungfish [14] and chondrichthyans [15] as they adapted to a post-extinction world.

The occurrence of probable plesiomorphic members of the Crassigyrinidae [2] and Colosteidae[8] indicates an inception 20-24 Myr earlier than the Late Mississippian as previously considered. Other tetrapod material, though of uncertain attributions, nevertheless demonstrates their distinctiveness, increasing known tetrapod diversity in the Tournaisian (**Extended Data Figs 1-6**).

Unusual among the discoveries of tetrapod specimens is the preponderance of small animals throughout the sequence, notably a very small tetrapod in a horizon 33 m above the D-C boundary, around 1 Myr after the extinction event (**Extended Data Fig. 1**). Of the five taxa described above, none has a skull length of more than 80 mm. This could indicate preservational or collector bias, but they are found throughout different lithologies, horizons and localities (**Extended Data Figs 1-6**). By contrast, larger tetrapod taxa are found at Willie's Hole, about one quarter of the way up the sequence, probably representing about 3 or 4 Myr above the ~D-C boundary. These results may challenge suggestions of a prolonged period of reduced body size in vertebrates following the DC extinction event [48]. Larger sizes seem to have appeared relatively rapidly in the Tournaisian, as also documented by trackways [43].

The earliest known pentadactyl limb is Tournaisian in age [2]. Differential adaptations to the ilium (Fig. 4), humeri, and femora [45] indicate progressive modifications to locomotory modes during the Tournaisian, also attested to by trackways that show a range of tetrapod sizes and gaits [43].

The tetrapods of the Ballagan have been found mainly in flood-generated sandy siltstones, but also in coarser more mixed sedimentary rocks associated with the base of fluvial channels or overbank flood deposits. The mosaic of closely juxtaposed floodplain environments, including pools, lakes, marshes, and areas of isolated woodland, may have provided the opportunity for both terrestrial and aquatic lifestyles in the monsoonal climate proposed for the early Carboniferous of northern Britain [49] and South Wales [50]. Whereas some parts of the flood plain were under water for long periods, others switched back and forth between palaeosols and bodies of standing water. This would suggest adaptation to both terrestrial and aquatic environments would be advantageous and thus advanced the radiation of tetrapods onto land. A recent study of the development of *Polypterus* shows how in early life, their skeletons can be differentially modified in response to exposure to water-based or land-based conditions. These results suggest that such skeletal flexibility might have contributed to the origin of tetrapod terrestrial morphology[51]. The varied environments of the Ballagan Formation may have encouraged such responses in early tetrapods.

Many different horizons through the Ballagan Formation in Scotland have yielded tetrapods, including at least 7 tetrapod-bearing horizons at Burnmouth (**Extended Data Fig. 1**) as well as three at Willie's Hole, with new tetrapod localities found at Tantallon Castle near North Berwick, the Heads of Ayr (**Extended data Fig. 6**) and Coldstream.

The wealth and diversity of tetrapod and arthropod taxa from the Tournaisian effectively refutes the proposal of a gap in the faunal fossil record, and our charcoal studies show that atmospheric oxygen levels, little different from those of either the Famennian or Viséan, were not a causal factor for the apparent gap. We emphasise the

356 importance of exploring or re-exploring Tournaisian sites elsewhere in the world, and
357 examining lithologies that may have been overlooked in the past.
358

359

360 References

361 1. Coates, M. I & Clack, J. A. Romer's Gap – tetrapod origins and terrestriality.
362 *Bull. Mus. Nat. Hist. Nat.* **17**, 373-388 (1995)
363 2. Smithson, T. R., Wood, S. P., Marshall, J. E. A. & Clack, J. A. Earliest
364 Carboniferous tetrapod and arthropod faunas from Scotland populate Romer's
365 Gap. *Proc. Natl. Acad. Sci. USA* **109,** 4532-4537 (2012)
366 3. Cohen, K.M., Finney, S.C., Gibbard, P.L. & Fan, J.-X. The International
367 Chronostratigraphical Chart, *Episodes* **36**, 199-204 (2013)
368 http://stratigraphy.org/ICSchart/ChronostratChart2016-04.pdf
369 4. Wood, S. P., Panchen, A. L. & Smithson, T. R. A terrestrial fauna from the
370 Scottish Lower Carboniferous. *Nature* **314**, 355-356 (1985)
371 5. Rolfe, W. D. I., Clarkson, E. N. K. & Panchen, A. L. (Eds). Volcanism and early
372 terrestrial biotas. *Trans. R. Soc. Edinb. Earth Sci.* **84**, (1994)
373 6. Milner, A. R. & Sequeira, S. E. K. The temnospondyl amphibians from the
374 Viséan of East Kirkton, West Lothian, Scotland. *Trans. R. Soc. Edinb. Earth Sci.*
375 **84**, 331-362 (1994)
376 7. Smithson, T. R., Carroll, R. L., Panchen, A. L. & Andrews, S. M. *Westlothiana*
377 *lizziae* from the Viséan of East Kirkton, West Lothian, Scotland. *Trans. R. Soc.*
378 *Edinb. Earth Sci.* **84**, 417-431 (1994)
379 8. Clack, J. A. *Gaining Ground: The origin and evolution of tetrapods.* 2nd Ed. 1-
380 523. (Indiana Univ. Press, 2012)
381 9. Ward, P. D., Labandeira, C., Laurin, M. & Berner, R. A. Confirmation of
382 Romer's Gap as a low oxygen interval constraining the timing of initial

arthropod and vertebrate terrestrialisation. *Proc. Natl. Acad. Sci. USA* **103**, 16818-16822 (2006)

10. Carroll, R. L., Belt, E. S., Dineley, D. L., Baird, D. & McGregor, D. C.Excursion A59, Vertebrate palaeontology of Eastern Canada. *24th International Geological Congress, Montreal* (1972)
11. Clack, J. A. & Carroll, R. L. in *Amphibian Biology, Vol. 4: Palaeontolog* (eds Heatwole, H. & Carroll, R. L.) 1030-1043 (Surrey Beatty, 2000)
12. Clack, J. A. An early tetrapod from 'Romer's Gap'. *Nature* **418**, 72-76 (2002)
13. Clack, J. A. & Finney, S. M. *Pederpes finneyae*, an articulated tetrapod from the Tournaisian of western Scotland. *J. Syst. Palaeont*. **2**, 311-346 (2005)
14. Smithson, T. R., Richards, K. R. & Clack, J. A. Lungfish diversity in Romer's Gap: reaction to the end-Devonian extinction. *Palaeontology* **59**, 29-44 (2016).
15. Richards, K. R., Sherwin, J. E., Smithson, T. R., Bennion, R. F., Davies, S. J., Marshall, J. E. A. & Clack, J. A. A new fauna of early Carboniferous chondrichthyans from the Scottish Borders. http://www.palass.org/meetings-events/annual-meeting/2015/annual-meeting-2015-cardiff-poster-abstracts (2015)
16. Clack, J. A. The dermal skull roof of *Acanthostega*, an early tetrapod from the Late Devonian. *Trans. R. Soc. Edinb. Earth Sci.* **93**, 17-33 (2002)
17. Jarvik, E. The Devonian tetrapod *Ichthyostega*. *Fossils and Strata* **40**, 1-206 (1996)
18. Smithson, T. R. The cranial morphology of *Greererpeton burkemorani* (Amphibia: Temnospondyli). *Zoo. J. Linn. Soc.* **76**, 29-90 (1982)
19. Lombard, R. E. & Bolt, J. R. *Sigournea multidentata*, a new stem tetrapod from the Upper Mississippian of Iowa, USA. *J. Palaeont*. **80,** 717-725 (2006)

20. Wilkinson, M. Coping with abundant missing entries in phylogenetic inference using parsimony. *Syst. Biol.* **44**, 501-514 (1995)

21. Goloboff, P. A. Estimating character weights during tree search. *Cladistics* **9**, 83-89 (1993)

22. Ruta, M., Coates, M. I. & Quicke, D. L. J. Early tetrapod relationships revisited. *Biol. Rev.* **78**, 251-345 (2003)

23. Ruta, M. & Clack, J. A. A review of *Silvanerpeton miripedes*, a stem amniote from the Lower Carboniferous of East Kirkton, West Lothian, Scotland. *Trans. R. Soc. Edinb. Earth Sci.* **97**, 31-63 (2006)

24. Klembara J., Clack, J. A. & Milner A. R. Cranial anatomy, ontogeny, and relationships of the Late Carboniferous tetrapod *Gephyrostegus bohemicus* Jaekel, 1902. *J. Vert. Pal.* **34**, 774-792. (2014).

25. Laurin, M. The evolution of body size, Cope's rule and the origin of amniotes. *Syst. Biol.* **53**, 594-622 (2004).

26. Marjanović, D. & Laurin, M. The origin(s) of extant amphibians: a review with emphasis on the "lepospondyl hypothesis". *Geodiversitas* **35**, 207-272. (2013)

27. Andrews, J. E., Turner, M. S., Nabi, G. & Spiro, B. The anatomy of an early Dinantian terraced floodplain: palaeo-environment and early diagenesis. *Sedimentology* **38**, 271-287 (1991)

28. Dormeier, M. & Torsvik, T. J. Plate tectonics in the Paleozoic. *Geosci. Frontiers* **5**, 303-350. (2014)

29. Belt, E. S., Freshney, E. C. & Read, W. A. Sedimentology of Carboniferous cementstone facies, British Isles and Eastern Canada. *J. Geol.* **75**, 711-721. (1967)

30. Bennett, C. E., Kearsey, T. I., Davies, S. J., Millward, D. Clack, J. A., Smithson,T. R. & Marshall, J. E. A. Early Carboniferous sandy siltstones preserve rare vertebrate fossils in seasonal flooding episodes. *Sedimentology* "Accepted Article"; doi: 10.1111/sed.12280 (2016)

31. Greig, D. C. *Geology of the Eyemouth district*. Memoir of the British Geological Survey, Sheet 34. (1988)

32. Astin, T. R., Marshall, J. E. A., Blom, H. & Berry, C. M. The sedimentary environment of the Late Devonian East Greenland tetrapods. In: *The terrestrialisation process: Modelling complex interactions at the Biosphere-Geosphere Interface* (eds Vecoli, M., Clément G. & Meyer-Berthaud, B.). *Geol. Soc. Spec. Publ.* **339**, 93-109 (2010)

33. Cressler, W. L., Daeschler, E. B, Slingerland, R. & Peterson, D.A. Terrestrialization in the Late Devonian: a palaeoecological overview of the Red Hill site, Pennsylvania, USA. In *The terrestrialisation process: Modelling complex interactions at the Biosphere-Geosphere Interface* (eds Vecoli, M., Clément G. & Meyer-Berthaud, B.). *Geol. Soc. Spec. Publ.* **339**, 111-128 (2010)

34. Wilson, H. M. & Anderson, L. I. Morphology and Taxonomy of Paleozoic Millipedes (Dipolopoda: Chilognatha: Archipolypoda) from Scotland. *J. Paleont.*,**78**, 169-184. (2004).

35. Garcia, W.J., Storrs, G.W. & Greb, S.F., The Hancock County tetrapod locality: A new Mississippian (Chesterian) wetlands fauna from western Kentucky (USA). *Geol. Soc. Am. Spec. Papers* **399**, 155-167 (2006)

36. Davies, N. S. & Gibling, M. R. The sedimentary record of Carboniferous rivers: Continuing influence of land plant evolution on alluvial processes and Palaeozoic ecosystems. *Earth-Sci. Rev.* **120**, 40-79 (2013)

457 37. Corenblit, D., Davies, N. S., Steiger, J., Gibling, M. R. & Bornette, G.
458 Considering river structure and stability in the light of evolution: feedbacks
459 between riparian vegetation and hydrogeomorphology. *Earth Surf. Proc. Land.*
460 **40**, 189-207 (2015)
461 38. Robinson, J. M. Phanerozoic atmospheric reconstructions: a terrestrial
462 perspective. *Palaeogeogr. Palaeocl.* **97**, 51-62 (1991)
463 39. Scott, A. J. & Glasspool, I. J. The diversification of Paleozoic fire systems and
464 fluctuations in atmospheric oxygen concentration. *Proc. Nat. Acad. Sci. USA*
465 **103,** 10861-10865 (2006)
466 40. Glasspool, I. J., & Scott, A. C. Phanerozoic concentrations of atmospheric
467 oxygen reconstructed from sedimentary charcoal. *Nature Geoscience.* 3, 627-630
468 (2010)
469 41. Glasspool, I. J., Scott, A. C., Waltham, D., Pronina, N. & Shao, L. The impact of
470 fire on the Late Paleozoic Earth system. *Front. Plant Sci.* **6**, 1-13 (2015)
471 42. Belcher, C. M., Yearsley, J. M., Hadden, R. M., McElwain, J. C. & Guillermo,
472 R. Baseline intrinsic flammability of Earth's ecosystems estimated from
473 paleoatmospheric oxygen over the past 350 million years. *Proc. Nat. Acad. Sci.*
474 *USA* **107**, 22448-22453 (2010)
475 43. Mansky, C. F. & Lucas, S. G. Romer's Gap revisited: continental assemblages
476 and ichno-assemblages from the basal Carboniferous of Blue Beach, Nova
477 Scotia, Canada. *Bull. New. Mex. Mus. Nat. Hist.* **60**, 244-273 (2013).
478 44. Sallan, L. C. & Coates, M. I. End-Devonian extinction and a bottleneck in the
479 early evolution of modern jawed vertebrates. *Proc. Nat. Acad. Sci. USA* **107,**
480 10131-10135 (2010)
481 45. Anderson, J. S., Smithson, T. R., Mansky, C. F., Meyer, T. & Clack, J. A. A

482 diverse tetrapod fauna at the base of Romer's Gap. *Plos One*
483 DOI:10.1371/journal.pone.0125446 (2015)
484 46. Hedges, S. B., Marin, J., Suleski, M., Paymer, M. & Kumar, S. Tree of Life
485 reveals clock-like speciation and diversification. *Mol. Biol. Evol.* **32**, 835-845
486 (2015)
487 47. Kumar S. & Hedges S. B. TimeTree2: species divergence times on the iPhone.
488 *Bioinformatics* 27:2023-2024 www.timetree.org (2011)
489 48. Sallan L. C. & Gallimberti, A. K. Body-size reduction in vertebrates following
490 the end-Devonian mass extinction. *Science* **350**, 812-815 (2015)
491 49. Falcon-Lang, H. J. The Early Carboniferous (Courceyan-Arundian) monsoonal
492 climate of the British Isles: evidence from growth rings in fossil woods. *Geol.*
493 *Mag.* **136**, 177-187 (1999)
494 50. Wright, V., Vanstone, S. & Robinson, D. Ferrolysis in Arundian alluvial
495 palaeosols: evidence of a shift in the early Carboniferous monsoonal system. J.
496 *Geol. Soc.* **148**, 9-12 (1991)
497 51. Standen, E. M., Du, T. Y. & Larsson, C. E. Developmental plasticity and the
498 origin of tetrapods. *Nature* **513**, 54-58. (2014) doi:10.1038/nature13708
499 52. Goloboff, P. A., Farris, J. S., & Nixon, K. C.. TNT, a free program for
500 phylogenetic analysis. *Cladistics* **24**, 1-13 (2008)
501 53. Carpenter, D. K., Falcon-Lang, H. J., Benton, M. J., & Henderson, E.
502 Carboniferous (Tournaisian) fish assemblages from the Isle of Bute, Scotland:
503 systematics and palaeoecology. *Palaeontology* **57**, 1215-1240 (2014)
504 54. Friedman, M. & Sallan, L. C. Five hundred million years of extinction and
505 recovery: a Phanerozoic survey of large-scale diversity patterns in fishes.
506 *Palaeontology* **55**, 707-742 (2012)

55. Scott, W. B. Nodular carbonates in the Lower Carboniferous, Cementstone Group of the Tweed Embayment, Berwickshire: evidence for a former sulphate evaporite facies. *Scot. J. Geol.* **22**, 325-345 (1986)

56. Turner, M.S. *Geochemistry and diagenesis of basal Carboniferous dolostones from southern Scotland* (Unpublished Ph.D. thesis, University of East Anglia, 1991)

57. Scott, W. B. *The sedimentology of the cementstone group in the Tweed basin: Burnmouth and the Merse of Berwick.* (Unpublished PhD Thesis, Sunderland Polytechnic 1971)

58. Barnet, A. J., Wright, V. P. & Crowley, S. F. Recognition and significance of paludal dolomites: Late Mississippian, Kentucky, USA. *International Association of Sedimentology Special Publications* **45**, 477-500 (2012)

59. Muchez, P. & Viaene, W. Dolocretes from the Lower Carboniferous of the Campine-Brabant Basin, Belgium. *Pedologie* **37**, 187–202 (1987)

60. Searl, A. Pedogenic dolomites from the Oolite Group (Lower Carboniferous),South Wales. *Geol. J.* **23**,157–169 (1988)

61. Vanstone, S. D. Early Carboniferous (Mississippian) palaeosols from southwest Britain: influence of climatic change on soil development. *J. Sediment. Petrol.* **61**, 445–457 (1991)

62. Wright, V. P., Vanstone, S. D. & Marshall, J. D. Contrasting flooding histories of Mississippian carbonate platforms revealed by marine alteration effects in palaeosols. *Sedimentology* **44**, 825–842 (1997)

63. Wood, G., Gabriel, A.M. & Lawson, J.C. Palynological techniques –processing and microscopy. 29–50 in: *Palynology: Principles and Applications, Volume 1.*

Principles. (eds) Jansonius, J. and McGregor, D. C. (American Association of Stratigraphic Palynologists Foundation, Texas, 1996).

64. American Society for Testing and Materials (ASTM). D2799 - 13. Standard test method for microscopical determination of the maceral composition of coal. in: *Annual book of ASTM standards section 5 – Petroleum products, lubricants, and their fossil fuels. Volume 05.06 Gaseous Fuels; Coal and Coke; Bioenergy and Industrial Chemicals from Biomass*. (West Conshohocken, PA, ASTM International. DOI**:** 10.1520/D2799-13 http://www.astm.org/Standards/D2799.htm (2013)

65. Hansen, K. W. & Wallmann, K. Cretaceous and Cenozoic evolution of seawater composition, atmospheric O_2 and CO_2: A model perspective. *Am. J. Sci.* **303**, 94–148 (2003).

66. Bergman, N. M., Lenton, T. M. & Watson, A. J. COPSE: a new model of biogeochemical cycling over Phanerozoic time. *Am. J. Sci.* **304**, 397–437 (2004).

67. Arvidson, R.S., Mackenzie, F.T. & Guidry, M. Magic: A Phanerozoic model for the geochemical cycling of major rock-forming components. *Am. J. Sci.* **306**, 135–190 (2006).

68. Berner, R. A. GEOCARBSULF: A combined model for Phanerozoic atmospheric O_2 and CO_2. *Geochim. Cosmochim. Ac.* **70**, 5653–5664 (2006)

69. Berner, R. A. Phanerozoic atmospheric oxygen: new results using the GEOCARBSULF model. *Am. J. Sci.* **309**, 603–606 (2009)

70. Tyson, R. V. *Sedimentary organic matter*. 1- 615. Chapman & Hall, London, (1995)

554 71. Scott, A. J. & Glasspool, I. J. Observations and experiments on the origin and
555 formation of the inertinite group macerals. *Internl J. Coal Petr.*, **70**, 53–66.
556 (2007)
557 72. Clack, J.A., Ahlberg P.E., Blom H., & Finney S.M. A new genus of Devonian
558 tetrapod from East Greenland, with new information on the lower jaw of
559 *Ichthyostega*. *Palaeontology* **55**, 73-86 (2012)
560 73. Milner, A. C. & Lindsay, W. Postcranial remains of *Baphetes* and their bearing
561 on the relationships of the Baphetidae (= Loxommatidae). *Zoo. J. Linn. Soc.* **122**,
562 211-235 (1998)
563 74. Clack J. A. *Pholiderpeton scutigerum* Huxley, an amphibian from the Yorkshire
564 coal measures. *Phil. Trans. Roy. Soc. Lond.* B **318**, 1-107 (1987)
565 75. Smithson T. R. The morphology and relationships of the Carboniferous
566 amphibian *Eoherpeton watsoni* Panchen. *Zoo. J. Linn. Soc.* **85**, 317-410 (1985)
567 76. Laurin, M. A redescription of the cranial anatomy of *Seymouria baylorensis*, the
568 best known seymouriamorph (Vertebrata: Seymouriamorpha). *Paleobios* **17l,** 1-
569 16 (1996)
570 77. Godfrey, S. J. Ontogenetic changes in the skull of the Carboniferous tetrapod
571 *Greererpeton burkemorani* Romer 1969. *Phil. Trans. Roy. Soc. Lond. B* **323**,
572 135-153 (1989a)
573 78. Godfrey, S. J. The postcranial skeletal anatomy of the Carboniferous tetrapod
574 *Greererpeton burkemorani* Romer 1969. *Phil. Trans. Roy. Soc. Lond. B* **323**, 75-
575 133 (1989b)
576 79. Hook, R. W. *Colosteus scutellatus* (Newberry) a primitive temnospondyl
577 amphibian from the Middle Pennsylvanian of Linton, Ohio. *Am. Mus.Novit.*
578 **2770**, 1-41 (1983)

579

This paper contains 9 items of Extended Data and 4 items of Supplementary Information

Supplementary Information contains

1 Supplementary Video file (.mov). This shows the skull of *Aytonerpeton* as a rotational view of the 3-D skull in the main text Figure 4.

2 Supplementary 3-D pdf. This shows the contents of the whole block containing *Aytonerpeton* including postcranial elements.

3 Supplementary pdf This give additional data such as plesiomorphies and other remarks on tetrapod specimens and their sedimentological context.

4 Supplementary Data. This contains a pdf of the character list and data matrix used in the cladistic analysis.

Extended Data contains

1-6 Figures of additional tetrapod specimens. The tetrapod fossils in this collection represent conservatively a sample of at least 7 new taxa, but possibly more. A further taxon is represented by NMS G.2012.39.22 ("Ribbo" in ref 2). The *Crassigyrinus*-like jaw UMZC 2011.9.1 in ref 2 may belong to one of those figured here, or to NMS G.2012.39.22, although the dermal ornamentation does not match that in any of them.

7 Three additional cladograms

8 Box plot of fusinite abundances from the Famennian – Visean.

9 Table 1. Fusinite abundances for the 127 samples from the Famennian-Visean, and those for the Willie's Hole samples.

Figure legends

605 **Figure 1. a-b** *Koilops herma* gen. et sp. nov. (NMS G. 2013.39/14). **a**, Photograph of
606 specimen, mainly preserved as natural mould. **b,** Interpretive drawing of specimen. **c-g,**
607 *Perritodus apsconditus* gen. et sp. nov. (UMZC 2011.7.2, part a). **c,** Photograph of main
608 specimen block. **d,** Reconstruction of lower jaw in external view, from scan data and
609 part and counterpart specimens. **e,** Reconstruction of lower jaw in internal view made
610 from scan data and part and counterpart specimens. **f,** Segmented model from scans of
611 lower jaw in internal view. **g,** segmented model from scans of lower jaw in internal
612 view. Colour code in **f**,: orange, dentary; red, adsymphysial plate; turquoise, part of
613 prearticular; yellow, first coronoid; blue, second coronoid; cerise, third coronoid; pink,
614 splenial; violet, angular; purple, prearticular; green, splenial; external bones greyed out.
615 In **g**, green, splenial. Scale bar in **a**, **b**, and **c**, 10 mm. Abbreviations: add foss, adductor
616 fossa; adsymph, adsymphysial; ang, angular; cor, coronoid; dent, dentary; ecto,
617 ectopterygoid; fro, frontal; intemp, intertemporal; jug, jugal; l, left; lac, lacrimal; llc,
618 lateral line canal; max, maxilla; oa, overlap area for pterygoid; pal, palatine; par,
619 parietal; pofr, postfrontal; porb, postorbital; pospl, postsplenial; preart, prearticular;
620 prefro, prefrontal; premax, premaxilla; psph, parasphenoid; pteryg, pterygoid; quad,
621 quadrate; quj, quadratojugal; surang, surangular; vom, vomer.
622
623 **Figure 2**. *Ossirarus kierani* gen. et sp. nov. (UMZC 2016.3) **a**, Photograph of complete
624 specimen. Leaders point to **b,** Map of skull bones. **c,** Drawing of right tabular,
625 supratemporal and a partial unidentified bone. **d,** Drawing of exoccipital. **e**, Drawing of
626 quadrate. **f,** Photograph enlargement of part of postcranial portion of specimen, **g,**
627 Drawings of left and right parietal bones placed in articulation, **h,** Drawing of jugal and
628 postorbital placed in articulation, **i,** Photograph of jugal. **j,** Photograph enlargement of
629 right humerus. Scale bar in **b** 10 mm, scale bars in **c-j** 5 mm. Abbreviations: clav,

clavicle; cleith, cleithrum; exocc, exoccipital; iclav, interclavicle; jug, jugal; par, parietal; porb, postorbital; quad, quadrate; r, right; rad, radius; sutemp, supratemporal; tab, tabular.

Figure 3. *Diploradus austiumensis* gen. et sp. nov. (UMZC 2015.55.4). **a,** Photograph of complete specimen. Scale bar 10 mm, **b,** Map of specimen showing distribution of elements, **c,** Drawing of right maxilla, **d,** Upper, interpretive drawing of specimen; lower, reconstruction of jaw in internal view. **e,** Drawing of parasphenoid. **f,** Drawing of right jugal in internal view. **g,** Drawing of skull table. **h**, Drawing of pterygoid in dorsal view. Scale bars in **b-h**, 5 mm. Abbreviations as for Figures 1 and 2 except for: nat mould popar, natural mould of postparietal.

Figure 4. *Aytonerpeton microps* gen. et sp. nov. (UMZC 2015.55.8). **a,** Still from micro-CT scan of block containing most of the specimen. **b**, interpretive drawing of right side of skull and palate. **c,** Stills from micro-CT scan of right lower jaw in (upper image) dorsal view and (lower image) mesial view. **d,** Still from micro-CT scan of right palate in approximately ventral view. **e**, Still from micro-CT scan of entire specimen in the main block. Arrows point to elements in **g**. **f,** enlargement of ilium in lateral (left image) and medial (right image) views. **g**, elements of hind limb. **c** and **d**: Note the sutures between pterygoid and marginal palatal bones, and the lower jaw bones, are tightly sutured and difficult to see in the scan. Abbreviations as for Figures 1 and 2, except for: lmar Meck fen, margin of Meckelian fenestra; nas, nasal; sym, symphysis; septomax, septomaxilla. Scale bars for all except **f** are 10 mm.

Figure 5. Two cladograms from TNT analysis. **a,** Single most parsimonious tree

obtained from implied weights search with k=3 (see text and Supplementary Data for details). **b,** strict consensus of four equally parsimonious trees obtained from implied weights search with k=4.

Figure 6. Sedimentary conditions and arthropods associated with the tetrapods. **a**, Palaeoenvironment of two of the tetrapod deposits. Left: Sedimentary log of partial section at Burnmouth with *Aytonerpeton* and *Ossirarus*, from 332 to 356 metres above the base of the Ballagan Formation. Between the sandstone units at the top and base of this section the sedimentary rocks comprise an overbank facies association. This succession records the transition from wet to dry conditions through time, with environments illustrated in the reconstructions for dry and wet periods (right). The tetrapod fossil-bearing horizons within this section are sandy siltstones. **b**, Helminthomorph diplopod from Burnmouth UMZC 2013.5. **c**, Scorpion from Willie's Hole, NMS G.2015.32. 848.

METHODS

Micro-CT data

Specimen UMZC 2016.3 *Ossirarus* and NMS G. 2013.39/14 *Koilops* and UMZC 2011.7.2a *Perittodus* were prepared mechanically with mounted needle, some matrix was removed from *Ossirarus* with a brush and water, consolidated where necessary with Paraloid B72. Specimens UMZC 2011.7.2a *Perittodus* and UMZC 2015.55.8 *Aytonerpeton* were scanned with Cambridge Tomography Centre µ-CT. Scan data:- *Perittodus*: Isotropic voxel size, 0.0444mm. Projections:1080, Filter: 0.25mm Cu, Xray kV:160, Xray µA: 70, Slices:1647. Exposure: 1000, Gain: 24 dB. UMZC 2015.55.8 *Aytonerpeton*: Isotropic voxel size: 0.0609mm. Projections: 1080, Filter: None, Xray

kV: 120, Xray μA: 125, Slices: 1789, Exposure: 1000, Gain: 24 dB. Scanner make: Nikon XTH225 ST.

Cladistic analysis

A new database of 46 taxa coded for 214 osteological characters (170 cranial, 43 postcranial), and was subjected to maximum parsimony analyses. It was compiled from scratch to include representative early tetrapods. Characters were drawn up to capture the features of the new taxa as far as possible in the context of the range of early tetrapods available for comparison. Most were drawn from recent analyses [22-24]. Some were reworded or reformulated and some rescored. They are arranged in alphabetical order grouped into regions of the anatomy **(Supplementary Information 3)**.

The data matrix was subjected to maximum parsimony analyses in TNT v. 1.1 [52]. Several experiments of taxon and character manipulation were carried out, as detailed below, with identical search protocols throughout. Given the size of the matrix, tree searches relied on heuristic algorithms, following a simple series of steps under the 'Traditional search' option in the 'Analyze' menu in TNT. Before each search, we modified memory requirements under the 'Memory' option in the 'Settings' menu. One hundred Mbytes of general RAM were allocated, and a total of 50,000 trees were selected as the maximum size of tree space for the exploration of alternative tree topologies. In the initial part of the 'Traditional search' ('Wagner trees' box ticked), we chose 10,000 replicates (random stepwise addition sequences of taxa), keeping a maximum of five trees at the end of each replicate, using the bisection-reconnection algorithm for tree branch swapping, and retaining all trees found at the end of all replicates. A new round of branch swapping was then applied to all trees retained from the initial search ('trees from RAM' box ticked). For each set of experiments, where

705 applicable, we summarized the results in the form of a strict consensus, a 50% majority-
706 rule consensus.
707 Using the search settings expounded above, we carried out three types of
708 parsimony analysis. The first parsimony analysis, employing all taxa and characters
709 from the original matrix, treated all characters as having equal unit weight (default TNT
710 option). The second analysis, again using all taxa and characters, was based on implied
711 character reweighting [21], briefly described as follows. Given a character, its implied
712 weight (W) is given by K / (K + M - O), where M and O represent, respectively, the
713 greatest number of character-state changes and the observed number of character-state
714 changes for that character. The constant of concavity (K) is an integer, the value of
715 which determines the most parsimonious trees as those trees for which W is maximized
716 across all characters. As the selection of K is arbitrary, we experimented with increasing
717 values (K = 3, 4, 5 and 10). We did not report details of searches with other K values, as
718 our goal was to establish whether the Tournaisian taxa showed stable positions within a
719 minimal range of implied weighting increments. However, we ran analyses with values
720 varying between 6 and 10, with mixed outcomes. In some cases, the Tournaisian taxa
721 are heavily reshuffled, in others the branching sequence of other groups revealed
722 implausible arrangements that, we feel, were dictated by varying amounts of homoplasy
723 in the data, although a proper characterization of this phenomenon requires further
724 testing. Topologies with K=10 are reported as an example.
725 In the third analysis, characters were reweighted by the maximum value (best fit)
726 of their rescaled consistency indexes, such as were obtained from the first analysis.
727 Statistical branch support was evaluated through character resampling via
728 bootstrap (resampling with replacement; ref.) and jackknife (resampling without
729 replacement, with 33% of characters removed; ref.), using 1000 replicates in each case

730 and collapsing nodes with less than 50% support.

731 Of all new Tournaisian taxa, only *Diploradus* appears in a maximum agreement
732 subtree (a taxonomically pruned tree showing only taxa for which all most parsimonious
733 trees agree upon relationships).

734 As for the implied weighting analysis, we found stable mutual arrangements for
735 most Tournaisian taxa with K = 3, 4 and 5. With K = 10, the branching sequence of
736 Tournaisian taxa differed from those found with smaller values. In addition, slightly
737 different branching patterns emerge for various early tetrapod taxa/groups following
738 different implied weighting searches. Below, we highlight key differences among
739 various tree topologies.

740 In trees generated with K = 3, 4 and 5, *Ossirarus*, *Perittodus* and *Diploradus*
741 emerge as increasingly crownward taxa, in that sequence, along the tetrapod stem group,
742 whilst *Aytonerpeton* and *Koilops* are placed among stem amphibians and are thus part of
743 the tetrapod crown group. *Ossirarus* is crownward of a (*Ventastega* + *Ichthyostega*)
744 clade, with *Ossinodus* placed either immediately anti-crownward of (K = 3), in a
745 polytomy with (K = 4), or immediately crownward of *Ossirarus* (K = 5). *Perittodus* is
746 the sister taxon to the Devonian *Ichthyostega*-like taxon *Ymeria*, and the (*Perittodus* +
747 *Ymeria*) clade forms the sister group to *Pederpes*. *Diploradus* is immediately crownward
748 of a (*Whatcheeria* + *Occidens*) clade, which in turn occurs crownward of (*Pederpes* +
749 (*Perittodus* + *Ymeria*)). However, the branching sequence of Carboniferous stem
750 tetrapods more crownward than *Diploradus* varies. Thus, in trees with K = 3, the
751 branching sequence includes *Crassigyrinus*, *Doragnathus*, (*Megalocephalus* +
752 *Baphetes*) and *Loxomma*. In trees with K = 4, the sequence includes only *Crassigyrinus*
753 and *Doragnathus*, whereas all baphetids form a clade on the amphibian stem
754 (*Megalocephalus* + (*Loxomma* + *Baphetes*)). In trees with K = 5, the baphetid clade is,

once again, on the amphibian stem, but the sequence of stem tetrapods crownward of *Diploradus* differs substantially, and includes (*Eucritta* + *Doragnathus*), *Sigournea* and *Crassigyrinus*. In trees from K = 3 and 4, the (*Aytonerpeton* + *Sigournea*) clade forms the sister group to a (*Koilops* + (*Tulerpeton* + (*Greererpeton* + *Colosteus*))) clade. In turn, this wider group joins temnospondyls on the amphibian stem, with *Caerorhachis* as a more immediate sister taxon. In trees from K = 5, *Aytonerpeton* is collapsed in a trichotomy with temnospondyls and the (*Koilops* + (*Tulerpeton* + (*Greererpeton* + *Colosteus*))) clade. With K = 10, the results match those from the second set of parsimony analyses (reweighting).

As for other tetrapod groups, the amniote stem undergoes little reshuffling in trees derived from different K values. The most noticeable difference among such trees is the placement of *Silvanerpeton* and *Gephyrostegus*, both of which are immediately crownward of the 'anthracosauroids' (*Eoherpeton* + (*Pholiderpeton* + *Proterogyrinus*)) but swap their positions as the first and second most crownward plesion after anthracosauroids.

With characters reweighted by the maximum value of the rescaled consistency index, we found three trees differing only in the relative positions of *Whatcheeria*, *Pederpes* and *Occidens*, all of which form a clade. In those trees, all new Tournaisian taxa appear on the tetrapod stem. In particular, *Aytonerpeton* and *Perittodus* are sister taxa, and together they join *Ymeria*. In crownward order, the sequence of stem tetrapods includes: *Acanthostega*, *Ossinodus*, *Ventastega*, *Ichthyostega*, *Ossirarus*, the (*Ymeria* (*Aytonerpeton* + *Perittodus*)) clade, the (*Whatcheeria*, *Pederpes*, *Occidens*) clade, *Diploradus*, *Doragnathus*, *Sigournea*, a (*Koilops* + (*Tulerpeton* + (*Greererpeton* + *Colosteus*))) clade, *Crassigyrinus*, and a baphetid clade. *Caerorhachis* and *Eucritta*

appear as the earliest diverging plesions on the amphibian and amniote stem groups, respectively.

Sedimentological and Environmental Interpretation

Sandy siltstones are defined as matrix-supported siltstones with 1-2 mm size clasts of siltstone, palaeosols and very fine sandstone derived from floodplain sediments30. The matrix is usually grey, but can be black (due to abundant plant fragments), green (derived from green palaeosols) or red (due to subsequent pedogenic modification of the sandy siltstone). The facies occurs every 3.5 metres throughout the Ballagan Formation and has a random bed thickness distribution, ranging from 0.2-140 cm. Beds were measured from the Norham Core in which 71% of the 140 sandy siltstone beds overlie either palaeosols or a desiccated horizon [30.] Abundant articulated or semi-articulated vertebrate fossils occur in this facies in the Burnmouth and Willie's Hole field sections.

Laminated siltstones were likely deposited in relatively short-lived floodplain lakes, based on their thickness and common pedogenic modification and/or brecciation. The dominance of actinopterygians and rhizodonts within these lakes indicates a brackish-freshwater salinity [53,54]. Diverse palaeosols and palynology suggest habitats including forest, scrubland, wetland and desiccating pools traversed by rivers (predominantly meandering channels) and saline-hypersaline lakes depositing cementstones and evaporites (Main text Fig. 6a) [27-31,55].

Elsewhere in the section, cementstones (dolomitic beds) and evaporites (gypsum-anhydrite) are interbedded on a metre to sub-metre scale [31,56,57]. Erosive-based, cross-bedded sandstone units (one to tens of metres thick) with basal conglomerate lags cut

802 into all other facies [31]. The lags contain disarticulated vertebrate material including
803 acanthodian, rhizodont and tetrapod bones [30].

804 The saline-hypersaline lake deposits in the Ballagan Formation have been
805 interpreted to represent brackish [27,56,57] marginal marine [29] or hypersaline[55]
806 conditions. Other dolomitic units from the Mississippian of the Scottish Borders are
807 interpreted as saline coastal marshes [58-62].

808

809 Charcoal Analysis

810 The DOM of the Ballagan and other targeted horizons was extracted by standard
811 palynological demineralisation techniques [63].

812 Measurement of maceral reflectance in oil was by means of a Zeiss UMSP 50
813 Microspectrophotometer, housed in the School of Ocean and Earth Science, National
814 Oceanography Centre Southampton, University of Southampton Waterfront Campus.
815 Measurements were made under standard conditions as defined by the International
816 Committee for Coal Petrology[64].

817 Model-based estimates of atmospheric oxygen concentration during the early
818 Tournaisian vary from 10 – 20%, with more recent models favouring the higher
819 figure[65-69]. As an alternative, fossil charcoal is used by several authors as a proxy for
820 atmospheric oxygen[38-41], as wildfire activity, and hence charcoal production, is
821 proportional to oxygen supply[42].

822 That wildfire activity (and hence charcoal production) is proportional to oxygen
823 supply is supported by controlled burning experiments[42], which have demonstrated that

824 when O_2 exceeds the present atmospheric level (PAL) of 20.9%, fire activity rapidly
825 increases and reaches a plateau at around 24%; therefore, fusain abundance is likely
826 insensitive to any further increase. The most comprehensive attempt thus far to
827 reconstruct Phanerozoic O_2 in this way[41] indicated 25.6% O_2 during Romer's Gap –
828 substantially higher than PAL and exceeding the presumed upper limit of 24%.
829 However, this study was based on the inertinite (= fusain) content of coals, which are
830 infrequent during the Tournaisian, so sampling density was relatively low. Furthermore,
831 we assume that large-scale forest fires will have a far greater influence on coal deposits,
832 formed *in situ* in forest mires, than on the more distal deposits of the kind examined
833 here.

834 The organic maceral fusinite is considered synonymous with charcoal and can be
835 distinguished from other maceral types by its reflectance under incident light[70]; we have
836 focused solely on fusinite for this study because, although most other members (semi-
837 fusinite) of the inertinite group are also accepted as pyrolitic in origin[71], their
838 reflectance forms a continuum between that of vitrinite and fusinite and forms the bulk
839 of the organic matter. This makes the % sum of semi-fusinite and fusinite very large
840 (>90%) and less reliable.

841 Twelve samples from the Willie's Hole locality were analysed for charcoal
842 content (Table 1). Mean abundance was 2.0%, which is within error of data obtained
843 from Burnmouth Shore, suggesting that the contribution from local fire activity (if any)
844 was similar at both sites (**Extended Data Table 1 and Extended Data Figure 8**).
845

846 Author contributions

JAC is corresponding author and lead PI and with TRS, JAC, BKAO, and KZS collected, described and analysed the tetrapod specimens. CEB, TIK, SJD and DM contributed to the stratigraphical, sedimentological and environmental studies. JEAM, DKC, and EJR contributed to the charcoal, palynological and stratigraphical studies. MR and JAC contributed to the phylogenetic analysis. AJR contributed information on the arthropods, SW provided additional work on micro-CT scan data. AJR, SAW and NCF organised the Willie's Hole excavation that provided sedimentological information. All authors contributed to discussion, preparation and writing the paper.

Acknowledgements

We acknowledge funding from NERC consortium grants NE/J022713/1 (Cambridge), NE/J020729/1 (Leicester), NE/J021067/1 (BGS), NE/J020621/1 (NMS), NE/J021091/1 (Southampton). We thank the following for their support and contributions. Stan and Maggie Wood for discovery of and access to collections, Oliver and Betty Kieran and Burnmouth community for support for the project, Mike Browne for field assistance and information on stratigraphy, Matt Lowe for access to collections, Sarah Finney for field assistance, conservation advice and preparation of *Koilops*, Vicen Carrió for conservation and preparation of NMS specimens, Janet Sherwin for stratigraphy and field assistance. Shir Akbari (Southampton) contributed to palynological processing. TIK and DM publish with the permission of the Executive Director, British Geological Survey (NERC). Anne Brown and Colin MacFadyen of Scottish Natural Heritage gave permission to collect at sites in their care, and Paul Bancks from The Crown Estates Office in Edinburgh, gave permission to collect on Crown land. PRISM, the Isaac Newton Trust Fund (Trinity College, Cambridge), the Crotch Fund (UMZC) and an anonymous donor provided funding for purchase of specimens. This is a contribution to

872 IGCP project 596.

873

874 Micro-CT will be deposited on the website Dryad following acceptance

875 Zoobank IDs will be obtained for the newly named taxa following acceptance

877 The authors declare no competing financial interests

878 Correspondence should be addressed to j.a.clack@zoo.cam.ac.uk

879

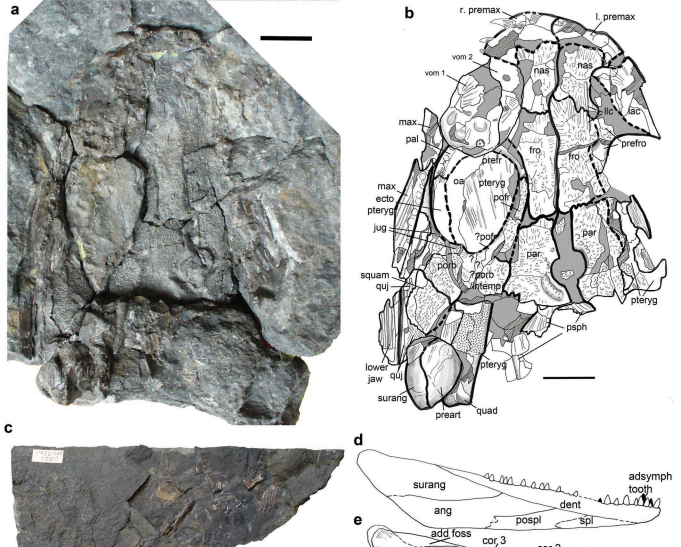

Figure 1. a-b) *Koilops herma* gen. et sp. nov. (NMS G. 2013.39/14). **a**, Photograph of specimen, mainly preserved as natural mould. **b,** Interpretive drawing of specimen. **c-g,** *Perritodus apsconditus* gen. et sp. nov. (UMZC 2011.7.2, part a). **c,** Photograph of main specimen block. **d,** Reconstruction of lower jaw in external view, from scan data and part and counterpart specimens. **e,** Reconstruction of lower jaw in internal vew made from scan data and part and counterpart specimens. **f,** Segmented model from scans of lower jaw in internal view. **g,** segmented model from scans of lower jaw in internal view. Colour code in **f,**: orange, dentary; red, adsymphysial plate; turquoise, part of prearticular; yellow, first coronoid; blue, second coronoid; cerise, third coronoid; pink, splenial; violet, angular; purple, prearticular; green, splenial; external bones greyed out. In **g**, green, splenial. Scale bar in **a**, **b**, and **c**, 10 mm. Abbreviations: add foss, adductor fossa; adsymph, adsymphysial; ang, angular; cor, coronoid; dent, dentary; ecto, ectopterygoid; fro, frontal; intemp, intertemporal; jug, jugal; l, left; lac, lacrimal; llc, lateral line canal; max, maxilla; oa, overlap area for pterygoid; pal,palatine; par, parietal; pofr, postfrontal; porb, postorbital; pospl, postsplenial; preart, prearticular; prefro, prefrontal; premax, premaxilla; psph, parasphenoid; pteryg, pterygoid; quad, quadrate; quj, quadratojugal; surang, surangular; vom, vomer.

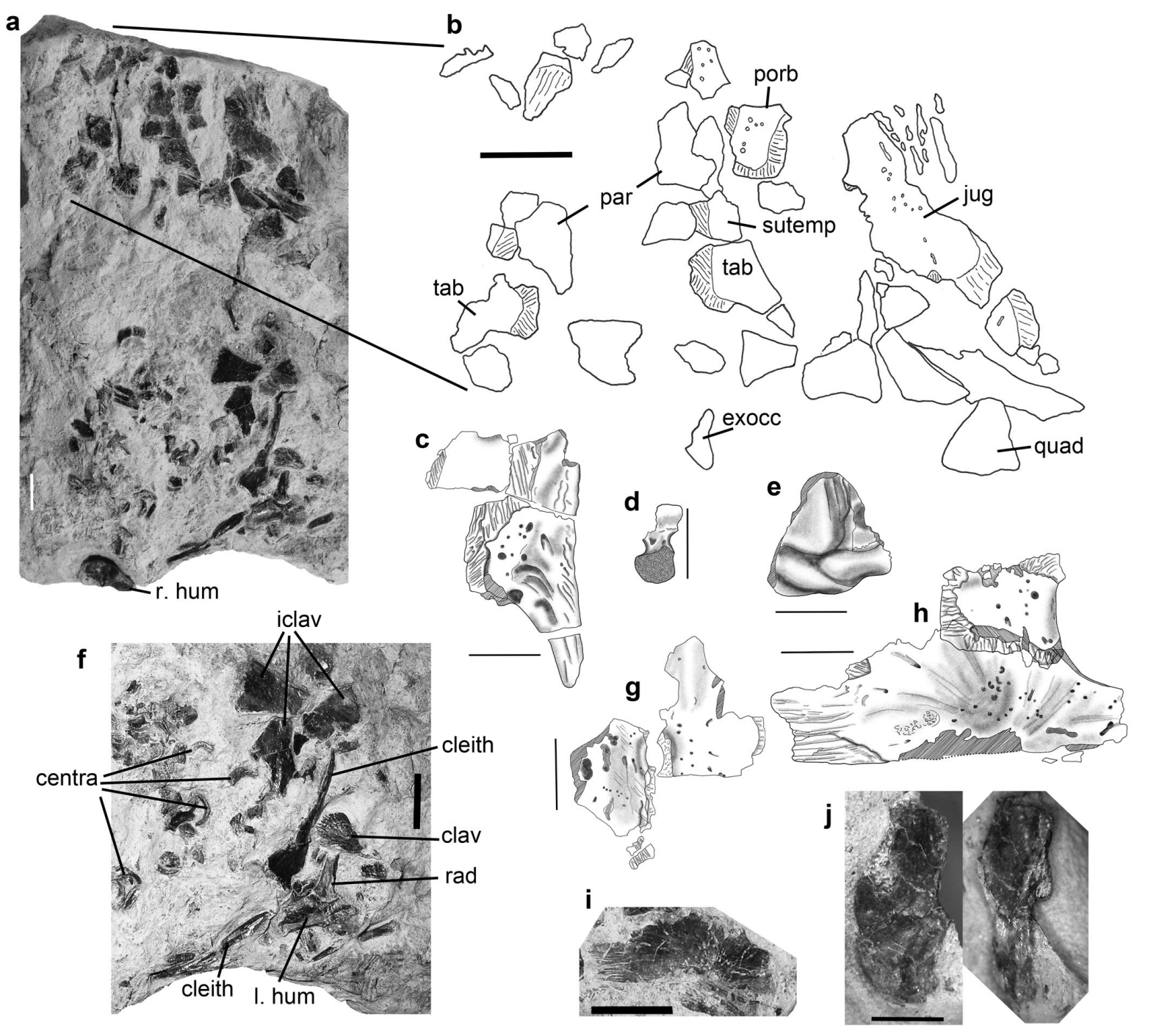

Figure 2. *Ossirarus kierani* gen. et sp. nov. TRS 2010.06.12.01, UMZC 2016.3. **a**, Photograph of complete specimen. Leaders point to **b,** Map of skull bones. **c,** Drawing of right tabular, supratemporal and a partial unidentified bone. **d,** Drawing of exoccipital. **e**, Drawing of quadrate. **f,** Photograph enlargement of part of postcranial portion of specimen, **g,** Drawings of left and right parietal bones placed in articulation, **h,** Drawing of jugal and postorbital placed in articulation, **i,** Photograph of jugal. **j,** Photograph enlargement of right humerus. Scale bar in **b** 10 mm, scale bars in **c-j** 5 mm. Abbreviations: clav, clavicle; cleith, cleithrum; exocc, exoccipital; iclav, interclavicle; jug, jugal; par, parietal; porb, postorbital; quad, quadrate; r, right; rad, radius; sutemp, supratemporal; tab, tabular.

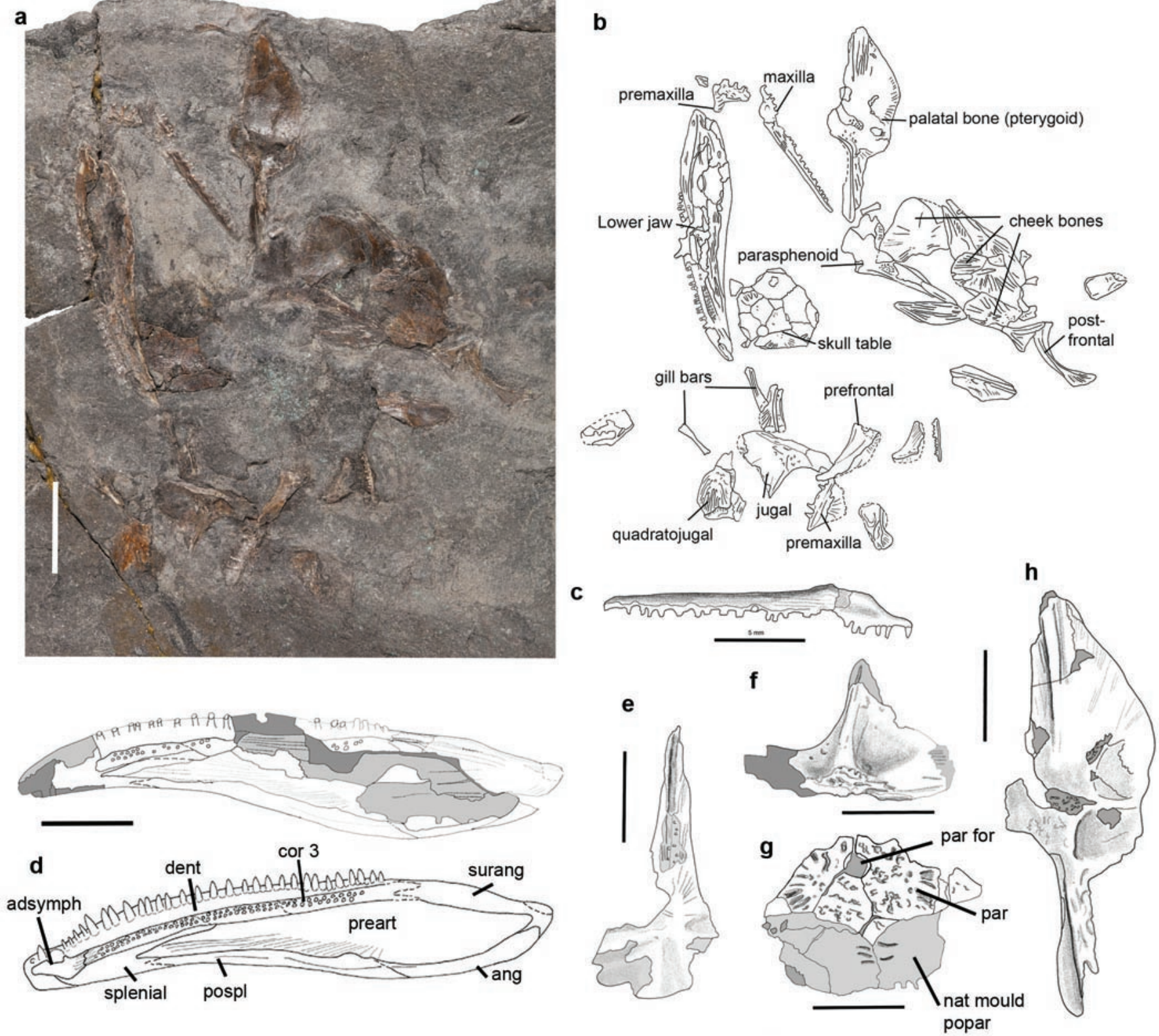

Figure 3. *Diploradus austiumensis* gen. et sp. nov. (UMZC 2015.55.4). **a,** Photograph of complete specimem. Scale bar 10 mm, **b,** Map of specimen showing distribution of elements, **c,** Drawing of right maxilla, **d,** Upper, interpretive drawing of specimen; lower, reconstruction of jaw in internal view. **e,** Drawing of parasphenoid. **f,** Drawing of jugal right jugal in internal view. **g,** Drawing of skull table. **h**, Drawing of pterygoid in dorsal view. Scale bars in **b-h**, 5 mm. Abbreviations as for Figures 1 and 2 except for: nat mould popar, natural mould of postparietal.

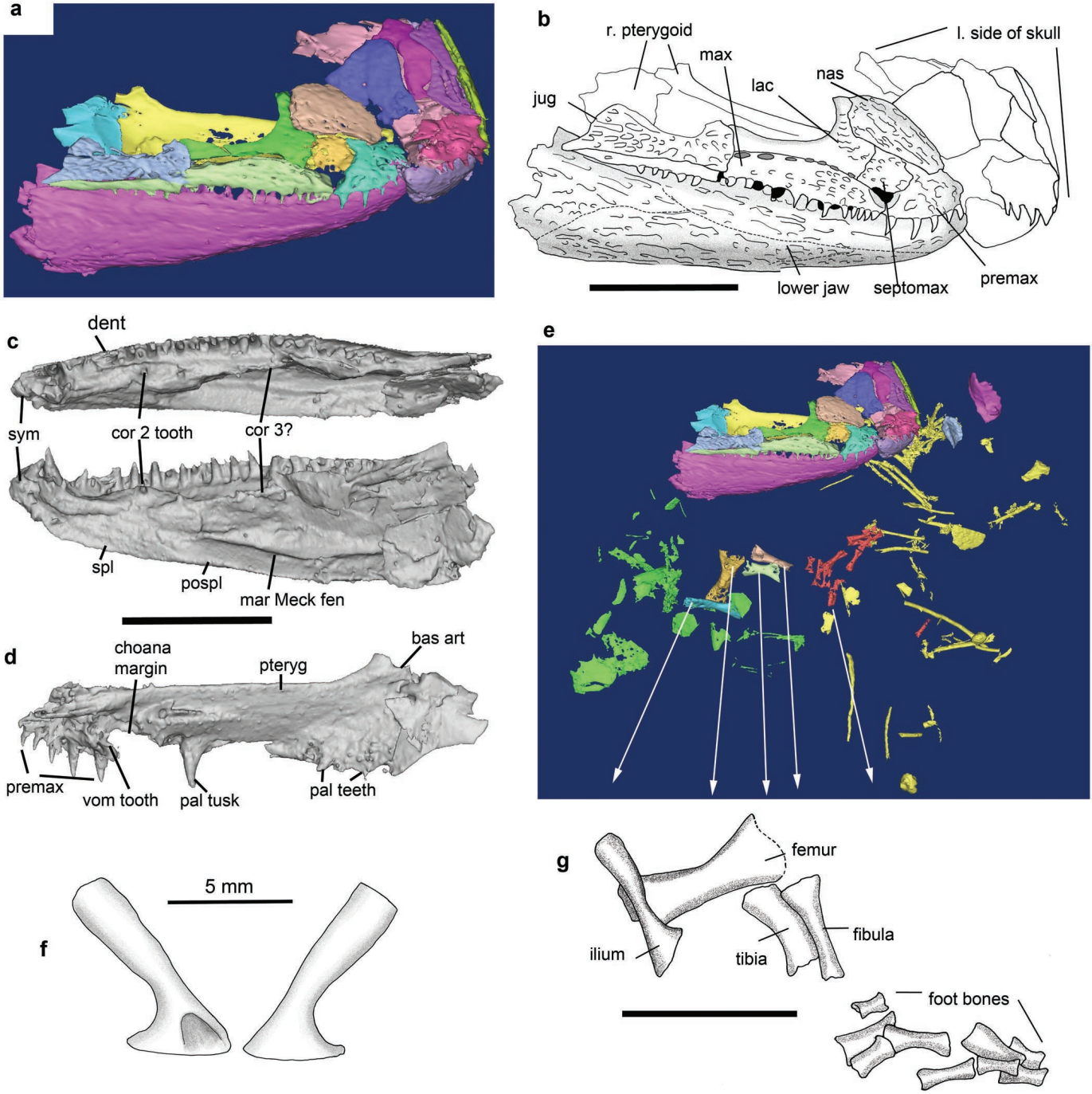

Figure 4. *Aytonerpeton microps* gen. et sp. nov. (UMZC 2015.55.8). **a,** Still from micro-CT scan of block containing most of the specimen. **b**, interpretive drawing of right side of skull and palate. **c,** Stills from micro-CT scan of right lower jaw in (upper image) dorsal view and (lower image) mesial view. **d,** Still from micro-CT scan of right palate in approximately ventral view. **e**, Still from micro-CT scan of entire specimen in the main block. Arrows point to elements in **g**. **f,** enlargement of ilium in lateral (left image) and medial (right image) views. **g**, elements of hind limb. **c** and **d**: Note the sutures between pterygoid and marginal palatal bones, and the lower jaw bones, are tightly sutured and difficult to see in the scan. Abbreviations as for Figures 1 and 2, except for: lmar Meck fen, margin of Meckelian fenestra; nas, nasal; sym, symphysis; septomax, septomaxilla. Scale bars for all except **f** are 10 mm.

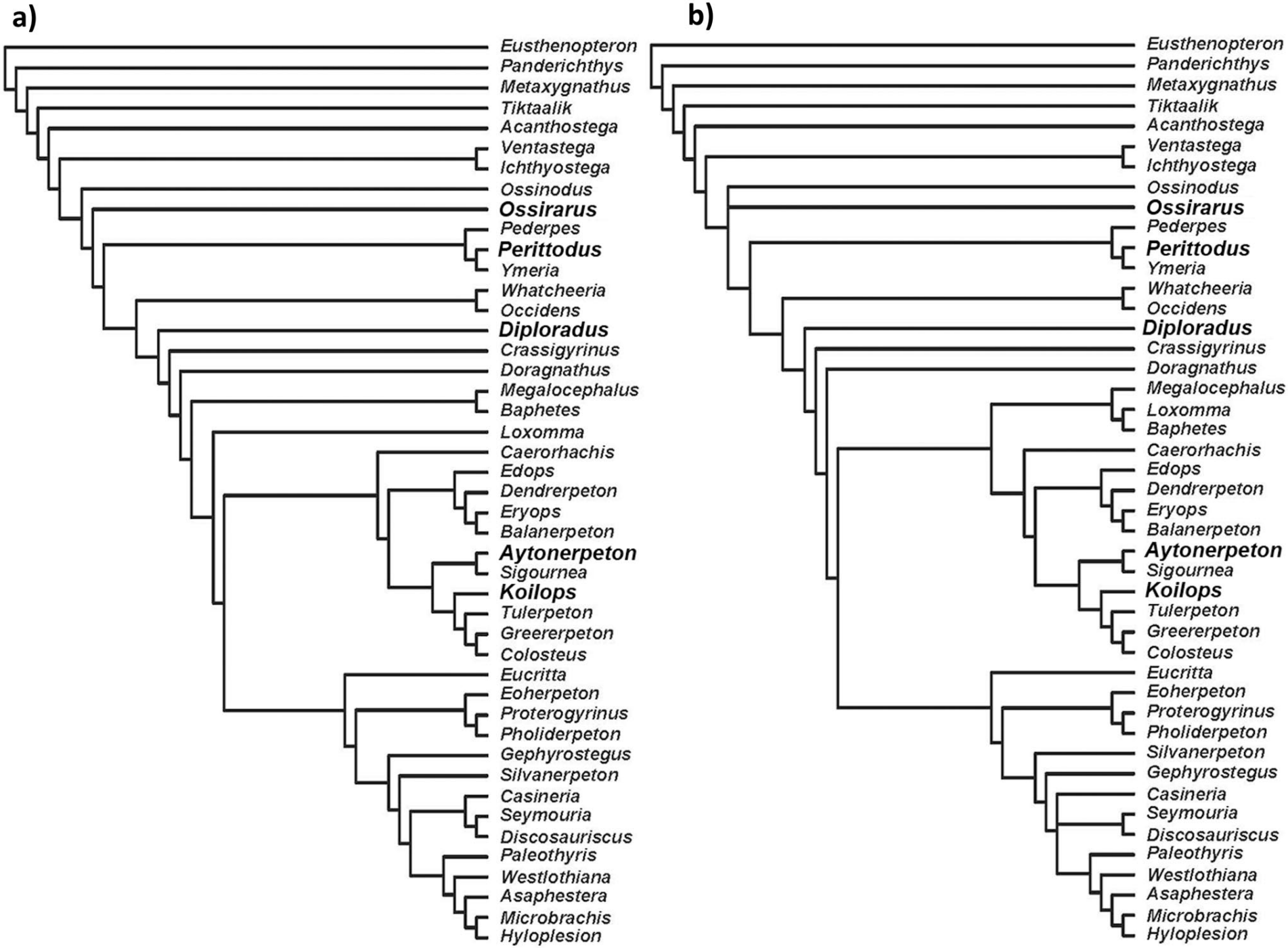

Figure 5. Two cladograms from TNT analysis. **a,** Single most parsimonious tree obtained from implied weights search with k=3 (see text and Supplementary Data for details). **b,** strict consensus of four equally parsimonious trees obtained from implied weights search with k=4.

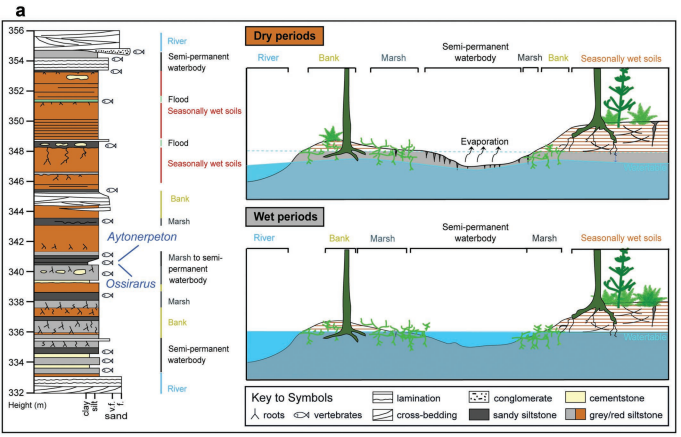

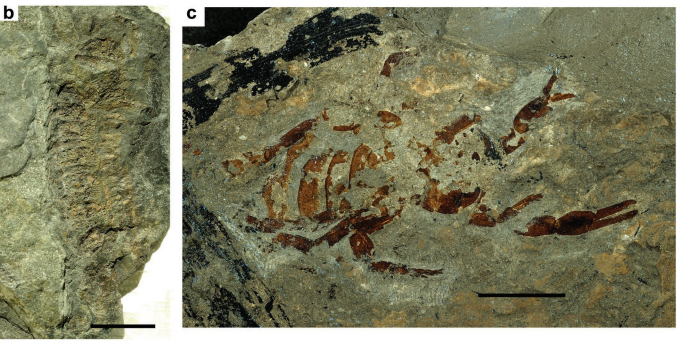

Figure 6. Sedimentary conditions and arthropods associated with the tetrapods. **a**, Palaeoenvironment of two of the tetrapod deposits. Left: Sedimentary log of partial section at Burnmouth with *Aytonerpeton* and *Ossirarus*, from 332 to 356 metres above the base of the Ballagan Formation. Between the sandstone units at the top and base of this section the sedimentary rocks comprise an overbank facies association. This succession records the transition from wet to dry conditions through time, with environments illustrated in the reconstructions for dry and wet periods (right). The tetrapod fossil-bearing horizons within this section are sandy siltstones. **b**, Helminthomorph diplopod from Burnmouth UMZC 2013.5. **c**, Scorpion from Willie's Hole, NMS G.2015.32. 848.